Article:

Kylafis, GF, Tomlin, AS orcid.org/0000-0001-6621-9492, Sleigh, PA orcid.org/0000-0001-9218-5660 et al. (2 more authors) (2018) The influence of dust originating from carbon black nanopowders on the explosion characteristics of lean methane/air mixtures within a turbulent environment. Journal of Loss Prevention in the Process Industries, 55. pp. 61-70. ISSN 0950-4230

https://doi.org/10.1016/j.jlp.2018.06.003

Title: The influence of dust originating from carbon black nanopowders on the explosion characteristics of lean methane/air mixtures within a turbulent environment.

Georgios F. Kylafis[a], Alison S. Tomlin[a], P. Andrew Sleigh[b], Malcolm Lawes[c], Alexis Vignes[c]

[a] School of Chemical and Process Engineering, University of Leeds, LS2 9JT, UK

[b] School of Civil Engineering, University of Leeds, LS2 9JT, UK

[c] School of Mechanical Engineering, University of Leeds, LS2 9JT, UK

[d] INERIS, Parc Technologique ALATA, B.P. 2, F-60550 Verneuil-en-Halatte, France

Keywords: Hybrid mixture explosions; engineered nanomaterials; methane; explosion hazard

Abstract

Industrial requirements present some unique challenges that can be met only by the application of engineered nanomaterials (ENMs). The completion of risk assessments based on the knowledge of the change in the explosion severity of turbulent gas/air mixtures caused by the accidental dispersion of nanopowders is vital before integrating such materials into existing systems. In this work, known amounts of selected carbon black nanopowders were mixed with methane near the lower-flammability-limit (LFL) to form hybrid mixtures of variable dust concentration. Mixtures were ignited in a 23 L cylindrical combustion vessel that allowed the control of isotropic turbulence through specially designed fans. The particle size distribution, the explosion pressure history and the flame speed derived from high speed Schlieren cine photographs, were measured. The influence of dispersed amounts of nanopowders on explosion severity was investigated by comparing the results with those obtained for pure methane-air explosions. Results indicated that the release of a relatively low mass of nanopowder into methane-air mixtures resulted in a more severe explosion than that of a higher amount. Also, despite the very low content of volatiles in the selected nanopowders, a hybrid mixture can be ignitable at an equivalence ratio well below the LFL of the gas. However this ignitability was shown to be related to the agglomeration state of powder in the dispersion phase, indicating that as the mean particle size decreases, a hybrid mixture with an extremely low content of flammable gas could be ignitable. From a risk assessment point of view,

these results may have great significance for specific industrial processes aiming to utilise ENMs.

1. Introduction

A dust explosion may occur as the result of dust particle suspension in air under confinement and the presence of an ignition source. The process industry through its development in time has periodically been stigmatized due to a number of hazardous explosions, some extremely severe (Eckhoff, 2003; Kuriechan, 2005; Vijayaraghavan, 2004). Despite significant research, the risks of dust explosions are still not well understood in industry, and dust explosions continue to occur (Worsfold et al., 2012).

As nanotechnology is a rapidly expanding technology and consequently production and use are very likely to increase in the coming years, a request for global guidance on their environmental and safety risks has emerged (Hansen, 2010). Engineered nanomaterials (ENMs) are widely used in various research and industrial fields (Pritchard, 2004), in the event of a large release of engineered nanoparticles (ENPs) into the atmosphere, an explosive dust cloud could be formed and ignite if the cloud is within the explosive dust concentration range and an ignition source is available. It has been shown experimentally that as the particle size decreases down to the order of 1-10 μm, the explosion severity of a dust cloud tends to increase (Eckhoff, 2012). If this were to be extrapolated into the nanometre range, extreme explosion rates are potentially to be predicted. However, the limited dispersibility of ultrafine particle powders, as well as the tendency in clouds of nano-size particles to coagulate, are two factors that may limit the dust explosion severity at the nanoscale (Eckhoff, 2012).

A hybrid mixture is the combination of a combustible dust and a flammable gas. According to Worsfold et al. (2012), within the form of a hybrid mixture, the dust may be present below its minimum explosion concentration (MEC) and the gas may be present below its lower flammability limit (LFL). The combination of both conditions may however create a potentially explosive mixture. Following Amyotte and Eckhoff (2010), explosion parameters such as the maximum explosion pressure (P_{max}) and the maximum rate of pressure rise $(dP/dt)_{max}$, have been found to be promoted and to be greater than for either the dust or the gas alone, although the latter has been shown to be more affected. Methane has been found to be less ignitable compared to other hydrocarbons due to the high energy required to break its C-H bonds. However, increased explosion risks have been reported in methane/dust mixtures by a number of studies (Liu et al., 2007; Pilao et al., 2006).

Mixtures of flammable gas and dispersed fractions of solid particles are frequently present in diverse industrial applications and their explosions are still not well understood (Torrado et al., 2016). Several works (Cashdollar, 1996; Garcia et al., 2011; Khalili et al., 2012; Pilao et al., 2006) have studied explosions in hybrid mixtures, although there are still unanswered questions about the phenomena involved. If we consider the average particle size of the dusts tested in these works, then relatively few studies have focused on hybrid explosions involving ENMs. Potential new explosion hazards may be present for processes where ENMs are utilised to enhance the efficiency of established techniques applied in industry.

In a recent study conducted by Abdelsalam et al. (2016), the effect of metallic nanoparticles such as Co, Ni and Fe, on biogas and methane production from anaerobic digestion of livestock manure was investigated. Additionally, Lu et al. (2016) examined the effects induced by the use of specific metallic nanoparticles as additives for promoting the catalytic activity of methane combustion. From these studies it is understood that the danger derived from accidental ignition of a reactive two-phase mixture is not confined only to coal mining industries, but through the increased use of ENMs, it is likely to spread to other industries. A balance must be achieved between increased use for enhanced product performance with safe and predictive handling and storage of these materials.

According to Turkevich et al. (2015), nano-carbons are confirmed mainly to belong to the dust explosion class St-1 which has been determined to characterise weak explosions (Bouillard et al., 2008). Due to the very low content of volatiles, the flame propagation mode of explosions involving carbon black (CB) nanopowders is exclusively described by heat transfer between the particles (Kosinski et al., 2013). So far, only two experimental works (Kosinski et al., 2013; Torrado et al., 2016) have investigated the explosion characteristics of flammable gas/air atmospheres mixed with dispersed amounts of CB nanopowders and they are thus the most relevant with respect to the present work.

Kosinski et al. (2013) focused on explosions of CB nanopowders under the addition of some quantities of propane in a 20 litre explosion vessel. The igniters used in this work were a 6 J electric spark discharge and 1 kJ chemical igniters. The results showed that for lean gaseous mixtures, the addition of nanopowders increased the P_{max} and $(dP/dt)_{max}$ explosion parameters. Similar trends were observed for rich gaseous mixtures. For the highest nominal dust concentration (500 g/m^3) no explosion was recorded, and according to the authors this could be attributed to high deposition of the suspended particles in piping and dispersion nozzles. The scanning electron microscope (SEM) images of the explosion residues revealed the formation of large agglomerates. This agglomeration makes the explosion study more complicated than it would be for individual particles.

Torrado et al. (2016), studied the influence of CB nanopowders (Printex XE2 and Corax N550) in methane-air mixture explosions conducted in a 20 litre spherical vessel. They also studied the effect of the initial turbulence by varying the ignition delay time (the time between the start of the air pulse for the injection of powder and the triggering of ignition). In their work, ignition at 100 J was utilised through the use of chemical igniters. The results indicated that when a only few percent of CB was added in lean methane-air mixtures, a slight increase of P_{max} and decrease of $(dP/dt)_{max}$, were observed.

Up to date, the explosion studies on dust clouds generated from the dispersion of ENMs, such as nanopowders, have utilised the standardised methodology for determining explosion severity through the measurement of pressure history in constant-volume bombs. The acquired pressure data has been used for a theoretical calculation of the flame velocity due to the lack of optical access associated with standard spherical vessels, such as the 20 litre sphere utilised so far in the study of nanopowders' explosivity. Therefore, it is important to obtain a knowledge of the experimentally measured turbulent flame velocity through optical techniques in gas mixtures containing dispersed amounts of ENMs that will allow a more integrated design of prevention/protection systems in industries promoting their applications.

Furthermore, the influence of dust in hybrid mixtures with a gas below its LFL has been discussed by Dufaud et al. (2009), while several indications that explosions can occur even at these low equivalence ratio (φ) values have been reported by Amyotte et al. (2007), Cashdollar (1996) and Cashdollar (2000). Attempts to ignite hybrid mixtures composed of propane and dispersed amounts of a CB nanopowder below the LFL of gas, have been conducted by Kosinski et al. (2013), however they reported that this ignition was not possible due to the negligible amount of volatiles in the tested nanopowder.

Knowledge of the change in the explosion severity of lean turbulent fuel-air mixtures induced by the dispersion of known amounts of ENMs, is vital for the completion of risk assessments related to processes taking place in industrial environments such as those described above. The objective of the current work is to quantify and gain a better understanding of the effects of dust particle size on the severity and likelihood of hybrid mixtures containing fractions of ENPs originating from specific nanopowders.

To this end, two types of selected CB nanopowders were dispersed in lean methane-air for the formation of hybrid mixtures with variable dust concentration in a cylindrical explosion vessel providing adjustable mechanical turbulence. Explosion tests were conducted under atmospheric conditions and triggered by a spark plug of low nominal ignition energy. The explosion severity was characterised through the measurement of the explosion pressure history and of flame speed derived from high speed Schlieren cine photographs. Also, the particle size characteristics in the explored dust clouds were determined. The influence of the selected nanopowders on explosion severity was investigated by comparison with results obtained for pure methane-air explosions. The explosion potential of hybrid mixtures of specific dust concentration and with methane below its LFL, was also investigated. Finally, for the same hybrid mixtures, the effect of ignition energy on their explosion characteristics was evaluated through the application of an ignitor providing relatively higher ignition energy than that of the spark plug.

2. Material and methods

2.1 Apparatus and methods

The present work was conducted with existing apparatus which has been previously used for studies of gaseous combustion. Fig. 1 shows a schematic of the combustion apparatus. This is described in detail in Atzler (1999), and, Atzler and Lawes (1998). It comprises a cast steel cylinder of 305 mm diameter and 305 mm length and its working volume is 23 litres. At each end, optical quality windows constructed from fused silica 150 mm diameter and 39 mm thick are fitted. The apparatus is equipped with four identical eight-bladed fans equally spaced around the central circumferential plane at 45° to the horizontal. The fans generate isotropic turbulence within the field of view of the windows and this has been fully characterized by Lawes (1987). Specifically, the root mean square (rms) turbulent velocity fluctuation u´ was found to be a linear function of fan speed according to:

$$u' = 0.0016\omega \tag{1}$$

where ω is the fan speed in rpm. In the present study, in respect of the dispersion state of powder immediately after its injection in the explosion vessel, we considered that the dispersed particles did not disturb the turbulence and that the turbulent velocity was directly imposed by the fan velocity. Furthermore, sufficient time (2 s) was provided between the end of injection and the start of ignition, for mixing purposes. Additionally, over the same period it was considered that the turbulent flow field generated by the transient dispersion process was suppressed by the uniform turbulence in the vessel imposed by the fans. Therefore, no influence was expected by the dust injection process on the validity of Eq. (1).

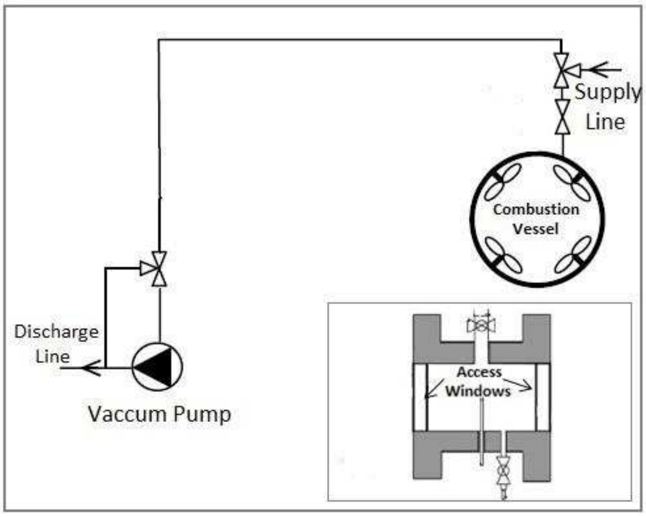

Fig. 1: Front view of the experimental apparatus (the inset graph illustrates the side view of the apparatus).

A commercially available stainless steel air cylinder (Humphrey 6-D-6 by Humphrey MI, USA) was used for the piston-cylinder device on which the injection of nanopowder samples into the explosion vessel was based. Some additions and modifications were made in order to adapt the device for this particular application and to prevent accidental spillages of the nanopowder samples on transferral from the fume-hood to the vessel. Fig. 2 shows the dust injector assembly and its components.

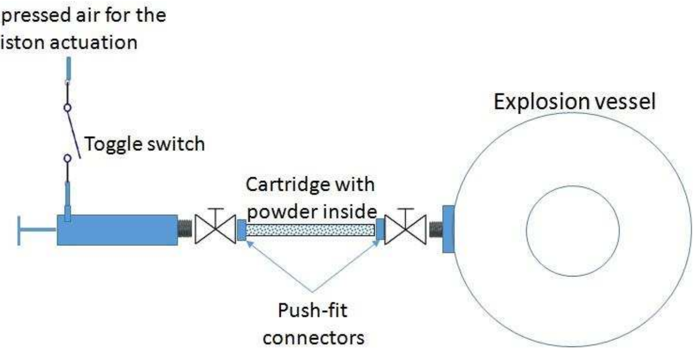

Fig. 2: Schematic of the dust injector assembly.

Prior to each explosion test, the chamber was evacuated to 50 mbar (a) and gaseous fuel was added by the partial pressure method, while the amount of nanopowder was derived from calculations of the volume based nominal dust concentration. The determined amount of nanopowder was introduced into the cartridge in a fume hood, and with the closed ball-valves attached the assembly was transferred to the explosion vessel where it was attached to the actuator unit. The ball valves were opened and the toggle switch was then actuated, allowing a burst of air at 7 bar to drive the piston and to generate a blast that promoted the dust particles into the vessel. After that, the ball valves were closed in order to isolate the system from combustion pressures and products, and then the mixtures were ignited by the ignition systems described below. The explosion tests presented in this work were conducted at atmospheric pressure and room temperature. Additionally, the rms velocity induced by the fans was adjusted to 0.8 m/s (500 rpm) for mixing purposes and subsequently for the conduction of turbulent explosions. It is assumed that both solid and gaseous fuels were well mixed with air during the injection process, prior to ignition. Higher fan speeds were not considered as dispersion tests at 1000 and 1500 rpm indicated that significant high quantities of the dispersed material deposited on the vessel’s internal surface, and subsequently that a very low quantity was able to remain suspended during the ignition process.

The turbulent mixtures were ignited by a standard 6.35 mm Minimag spark plug. This was mounted in the centre of the vessel using a stainless steel tube spark holder in which was mounted an insulated high voltage lead. The spark plug was connected to a variable energy ignition power supply unit. Due to the very low equivalence ratios (φ) used throughout this work, we used the highest possible ignition energy provided by the particular device (2 J). The ignitor effect is more important for the early stages of the explosion tests, and it is expected to be more significant in small explosion chambers (Zhen and Leuckel, 1997). According to Bradley and Lung (1987), the flame speed enhancement induced by a spark plug of 1 J has been observed at radii up to about 10 mm. It is expected that in this work the effect of 2 J on the phenomenology of flame will not be considerable, therefore this has been ignored in the Schlieren-based flame speed analysis by excluding the images corresponding to the early stage of the flame development.

In order to study the effect induced by the increase of the ignition energy on the explosion characteristics of a hybrid mixture with φ within the range below the LFL of gas, electric igniters supplied by Easypro (UK) were utilised and they were installed at the centre of the vessel. Calculations over three matches, based on the assumption of the completed combustion of pyrogen and on its heat of explosion (HOE) parameter, indicated that the energy corresponding to the mass change of match after ignition was 67 ± 4 J.

A piezoelectric pressure sensor (Kistler 701A), which was mounted flush with the inner surface at the bottom of the vessel, measured the pressure evolution inside the chamber during the explosion processes. The most important parameters obtained from the acquired pressure data were the maximum explosion pressure (P_{max}) and the maximum rate of pressure rise $(dP/dt)_{max}$.

The growth rate of the spherically expanding turbulent flames was studied using high speed Schlieren cine photography. This technique allows for the visualisation of density gradients and it has proved to be an effective method for flame imaging in combustion studies providing high-fidelity data for validation and further development of modelling and simulation approaches (Sick, 2013). The arrangement of the Schlieren cine photography system applied in this work is shown in Fig. 3. Schlieren images were captured using a Phantom V9.0 camera, recording at a rate of 3000 frames per second (FPS) at a resolution of 512 x 512 pixels. This produced greyscale images, with these being captured until the flame edge had reached the edge of the vessel windows. It should be noted that during an explosion test the pressure rise in the vessel during the Schlieren capture is negligible, as the direct flame measurement is based on the early stage of explosion when the flame develops within the region where optical access is provided by the vessel's windows. After that, the pressure in the vessel continues to increase and the obtained explosion pressure parameters (P_{max} and dP/dt_{max}) correspond to the stage when the flame has been stabilised within the vessel and has already passed out from the region where optical access is provided. Therefore, each measurement method describes a different aspect of the explosion.

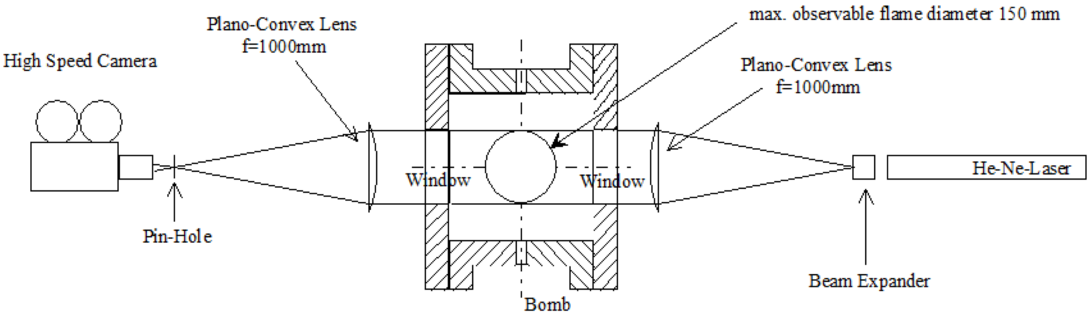

Fig. 3: Experimental apparatus for Schlieren flame photography.

It was necessary to ensure that the ignition system, high speed camera and pressure data acquisition system were triggered at a consistent point in time relevant to each other. To this end, a TGP110 pulse generator was used to generate the variety of signals required by these components. Through proper adjustments, the aforementioned components were able to be triggered simultaneously. Further details regarding each component constituting the experimental setup are described elsewhere (Kylafis, 2016).

2.2 Data processing techniques

A processing technique developed and applied by Mansour (2010) was employed in this work for the calculation of flame speeds based on the Schlieren images. The particular technique was initiated by conversion of original Schlieren cine movies acquired from the Phantom V9.0 camera into separate 8-bit bitmap image files through a number of MATLAB automated batch processing tools. This was followed by the subtraction of a pre-kernel image from each flame image to obtain a flame image without the intruding spark plug. Then the images were binarised to yield a white flame image, as can been seen in Fig. 4, surrounded by a black background. Specifically, the white and black represent flame and unburned gas respectively. The MATLAB script was then used to count the number of white pixels in each image and subsequently to calculate the radius of a circle with the same area, which was used to represent a mean flame radius. Flame speeds were then determined by plotting flame radius versus time during the explosions.

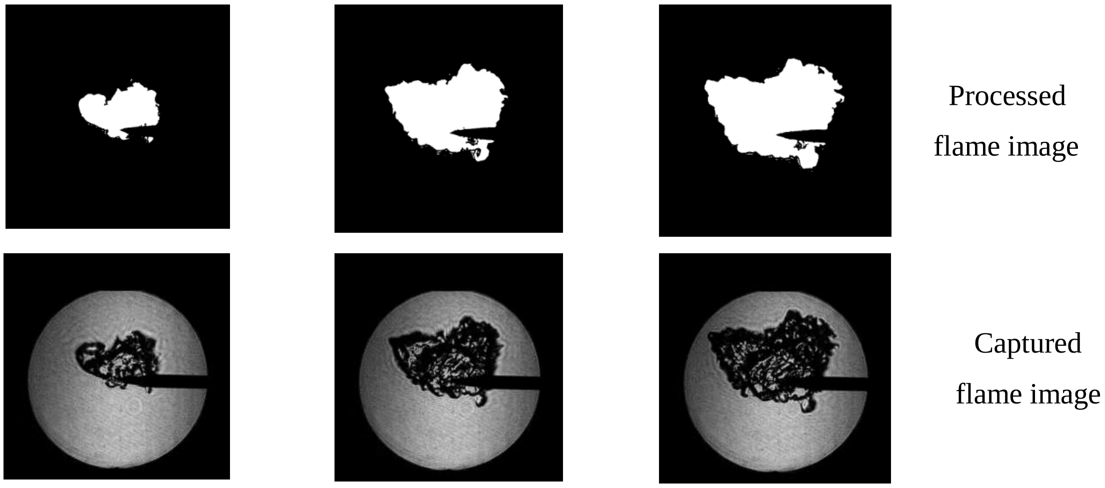

Fig. 4: Sequences of Schlieren images of flames of a typical methane-air turbulent explosion at φ = 0.68.

2.3 Particle size distribution analyser

The particle size characteristics in the dust clouds explored in the explosion tests, were determined by a differential mobility spectrometer (DMS500 by Cambustion Ltd., UK) sampling the air at the centre of chamber through an access port by means of a ¼ inch stainless steel pipe, under conditions identical to those applied in the explosion tests. The particular device classifies particles in the size range 5-1000 nm based on their mobility in an applied electric field. Based on the maximum response time of the instrument (200 ms) and on the calculated time between the end of dispersion and the activation of ignition (approximately 1 s), the measured particle size distributions (PSDs) were averaged over the specified duration in order to obtain an approximation of the particle size characteristics when ignition occurred.

2.4 *Experimental material's characteristics*

The CB used in the explosion tests was of types Corax N550 and Printex XE2 from Orion Engineered Carbons (Germany) with Brunauer-Emmett-Teller (BET) specific surface area 40 and 950 m^2g^{-1}, and with apparent bulk density 0.38 and 0.15 gm^{-3}, respectively. Both materials are specified by the manufacturer to have very low volatiles content (< 0.5 %), whereas both materials are described by a wide distribution of particle sizes with large agglomerates of several μm size, as confirmed by the scanning electron microscopy (SEM) analysis conducted in this work (Fig. 5). These μm agglomerates consist of primary particles with sizes ranging between 35-80 nm and 40-60 nm, for Corax N550 (Fig. 5a) and Printex XE2 (Fig. 5b), respectively.

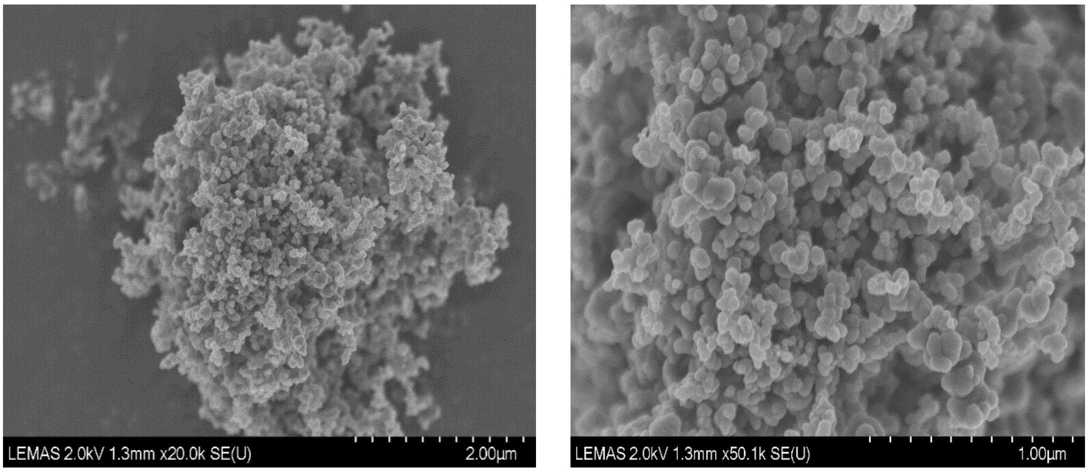

(a) Corax N550

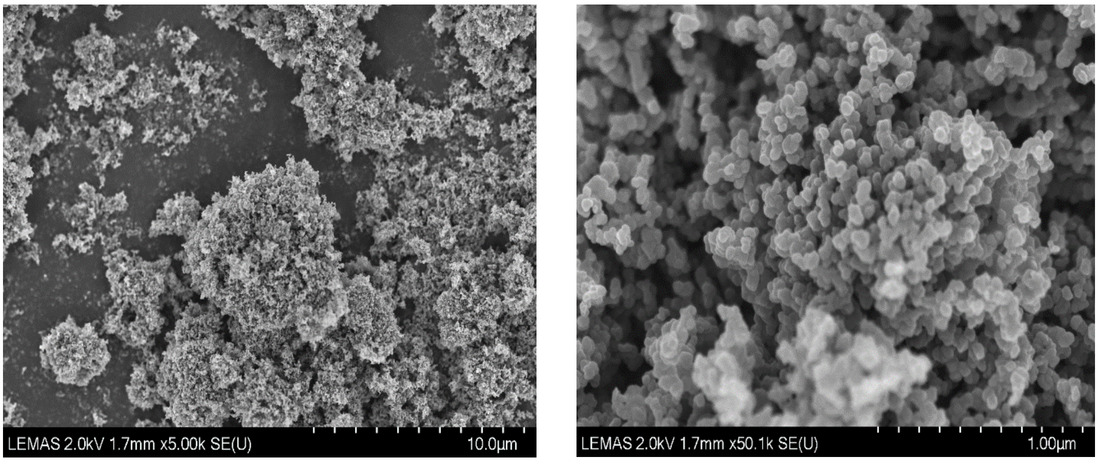

(b) Printex XE2

Fig. 5: SEM images of (a) Corax N550 and (b) Printex XE2 nanopowders.

3. Results and discussion

3.1 Dispersion experiments and particle size characterisation

A course of (no explosion) dispersion experiments was conducted in order to determine the particle size characteristics in the dust clouds explored in the explosion tests. The averaged PSD over the three runs, as well as the PSD measured for each run, are illustrated in Figs. 6 and 7, for Corax N550 and Printex XE2, respectively. It should be noted that the PSDs by number are presented as $dN/dlogd_P$ per cubic centimeter, where dN is the number of particles detected in a size channel and $dlogd_P$ is the difference between the logarithms of the upper and lower channel diameters. In the same figures, after grouping the total results into fine (> 100 nm) and ultrafine particles (≤ 100 nm), the modal fractions corresponding to the specified size categories can be seen for each tested powder concentration. Finally, a difference between the highest powder concentrations corresponding to each type of CB (75 and 37.5 gm^{-3}, for Corax N550 and Printex XE2, respectively), can be seen. As outlined in the previous section, these two types of CB demonstrate different apparent bulk densities (0.38 and 0.15 gm^{-3}, for Corax N550 and Printex XE2, respectively). To achieve the dispersion of 75 gm^{-3} of Printex XE2, it was necessary to introduce into the injector's catridge approximately double the mass compared to that required for the dispersion of 75 gm^{-3} Corax N550. In the subsequent explosion tests such a concentration of Printex XE2 caused the failure of the spark plug due to the high deposition of particles on the spark electrodes. Therefore, the nominal concentration of the particular material was adjusted to 37.5 gm^{-3} in order to ensure the fuctionality of the spark plug during the main explosion experiments.

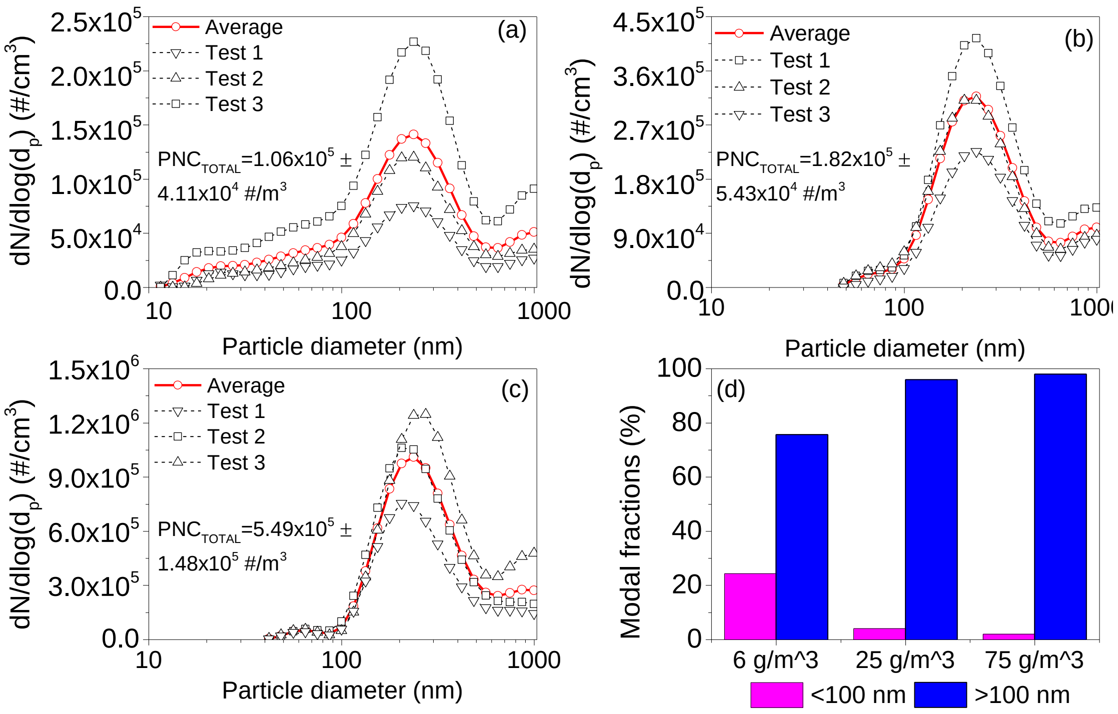

Fig. 6: PSDs measured by the DMS for (a) 6 gm^{-3}, (b) 25 gm^{-3}, and (c) 75 gm^{-3} of Corax N550 and (d) average modal fractions of the measured PSDs grouped into fine and ultrafine nanoparticles averaged over three replicate runs per dust concentration.

As shown in Figs. 6a-c, the measured PSDs for Corax N550 demonstrate broad multimodal characteristics with a main peak diameter at 237 nm, independent of the powder concentration. This diameter is larger than that of the primary particle size (35-80 nm), and substantially lower than that of the microscale agglomerates in the bulk form, suggesting that a large fraction of the latter were de-agglomerated into a size within the nanoscale by injecting the powder samples. Reasons for this may include the blast induced by the injection piston movement and/or interaction with the gaseous mixture through jet and turbulent shear forces. Additionally, it can be seen that all the PSDs of the different powder concentrations present a rise over the largest size channels of the DMS. This is an indication of a peak within the microscale, located very close to the nanoscale. However, micrometric PSD measurements were not possible in this work; therefore the accurate location of this peak was not identifiable.

Regarding the modal fractions (Fig. 6d), a negative association between the population of ultrafine particles and the increase of the nominal dust concentration, can be observed. It is important to note that the fraction of ultrafine particles in the dust cloud generated by the lowest dust concentration (6 gm^{-3}) was substantially higher than those in the dust clouds generated by the higher dust concentrations (25 and 75 gm^{-3}). Based on aerosol studies (Rim et al., 2012; Seipenbusch et al., 2008), this is quite reasonable as the coagulation effect is greater for small particles than for larger particles resulting in their fast disappearance at high number concentrations.

The dispersion of Printex XE2 (Fig. 7) resulted in total PNCs higher than those measured in the Corax N550 dispersion tests, as higher masses of the former were required in order to approximate the nominal dust concentrations applied in the dispersion tests of the latter. As shown in Figs. 7a-c, the general shape of the distribution function is broad and multimodal having a main peak diameter at 205 nm. In contrast to the Corax N550 dispersion tests, by increasing the mass of powder in the injector’s cartridge, a gradual decline of the size distributions over the larger size channels of DMS, can be seen. This trend indicates that a peak in the microscale was gradually distanced from the nanoscale by increasing the mass of the tested material, and subsequently that μm particles in the Printex XE2 dust clouds were larger than those in the Corax N550 ones.

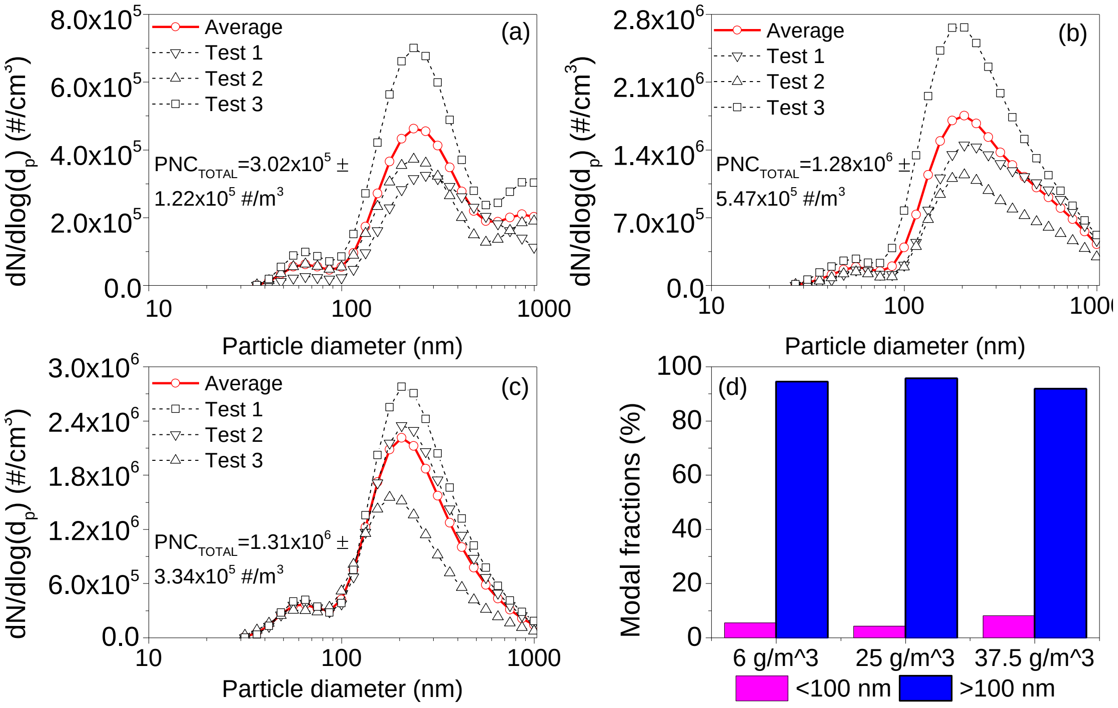

Fig. 7: PSDs measured by DMS for (a) 6 g/m^3, (b) 25 g/m^3, and (c) 37.5 g/m^3 of Printex XE2 and (d) the average modal fitting fractions of the measured PSDs grouped into fine and ultrafine nanoparticles averaged over three replicate runs per dust concentration.

Finally, Fig. 7d shows that the fraction of the Printex XE2 particles in the ultrafine range was smaller than that of the Corax N550 ones, at the lowest nominal dust concentration (6 gm^{-3}). On increasing the dust concentration this fraction was shown to continue being low and was independent of the amount of the injected dust which was not the case for Corax N550.

The indication that μm particles in the Printex XE2 dust clouds were larger than those in the Corax N550 ones, can be confirmed through the visualisation provided by the Schlieren system. Fig. 8 presents two Schlieren images randomly selected immediately after the dispersion of 25 gm^{-3} of each material. The image corresponding to Printex XE2 shows a significant increase in the concentration of black dots (large μm-particles) compared to that corresponding to Corax N550.

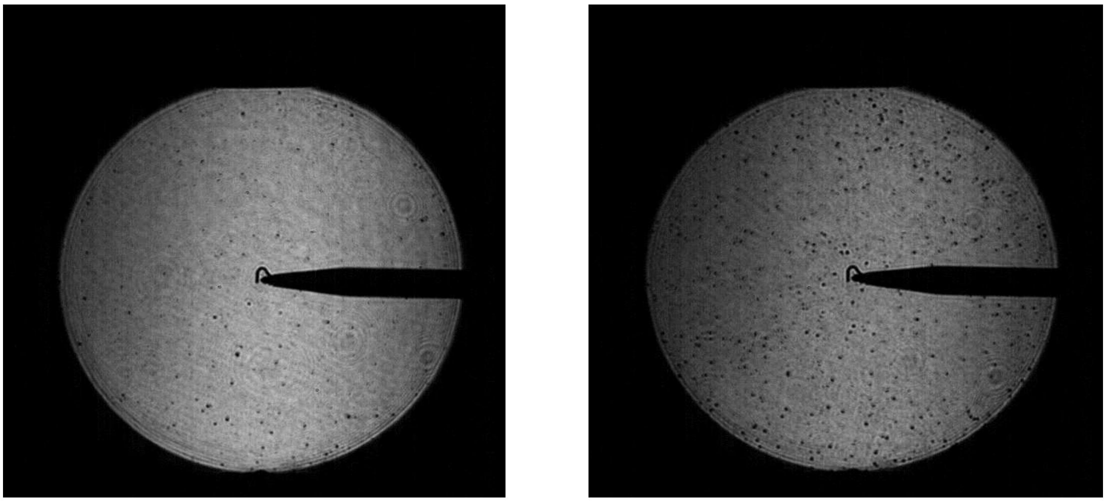

Fig. 8: Schlieren images of dispersed powders in the explosion vessel obtained for 25 gm^{-3} Corax N550 (left); $25gm^{-3}$ Printex XE2 (right).

3.2 Flammability of methane

In this series of explosions tests, the flammability of methane under the experimental conditions applied throughout the total number of tests performed in this work, was studied. Shown in Fig. 9 are the variations of the averaged P_{max} and the $(dP/dt)_{max}$ parameters respectively, over three repeats conducted for each condition, with the change of equivalence ratio. It should be stressed that the standard deviation of the pressure data over the total number of tests was ±1.63 and ±11.6 for P_{max} and (dP/dt_{max}) respectively. As can be seen, both the explosion parameters increased with increasing equivalence ratio towards stoichiometric, but there is a minimum equivalence ratio of 0.65 below which combustion could not be initiated.

The work of Cashdollar et al. (2000) indicated that under quiescent and atmospheric conditions in a 120 L chamber, the LFL for upward flame propagation of spark plug ignited methane in air was 5±0.1 % v/v, corresponding to $\varphi=0.55$. However, Abdel-Gayed et al. (1979), who explored the methane LFL at different fan speeds in the same explosion vessel used in the present work, reported that at the set conditions applied herein, mixtures were ignitable down to $\varphi=0.64$, with ignition limits (upper and lower) becoming gradually narrowed on increasing turbulence. Furthermore, the repeatable ignition in methane-air mixtures under the specified starting conditions was guaranteed at $\varphi=0.68$. Below this limit, it was not certain that the mixture would ignite. For this reason $\varphi=0.68$ was chosen as the condition into which were introduced

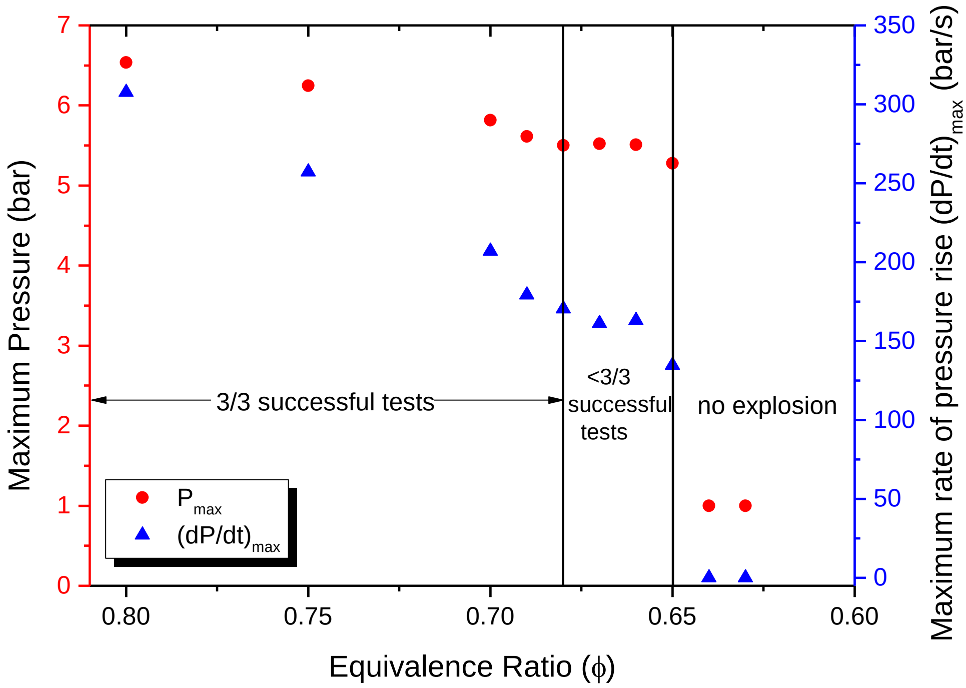

Fig. 9: The variation of average maximum explosion pressure (P_{max}) and average maximum rate of pressure rise ($(dP/dt)_{max}$) of methane-air mixtures, with equivalence ratio (φ). Note that the x-axis has been plotted in reverse order to illustrate the sequence of the experiments.

the nominal concentrations of dust from the two CB nanopowders, for ignitions through the spark plug and for the subsequent comparisons of the explosion parameters between heterogeneous and their respective homogeneous mixtures.

3.3 Explosions with methane (φ>LFL) and dispersed amounts of CB nanopowders

As indicated in the previous section, for φ = 0.68, three nominal dust concentrations of each tested material were introduced into methane-air to form hybrid mixtures. Interspersed in-between the tests on the hybrid mixtures, explosion tests on particle-free methane-air were conducted. The influence of the dispersed amounts of nanopowders on explosion severity was investigated by comparing the results obtained for the pure methane explosions.

Figs. 10 and 11, show the comparisons between the average explosion pressure characteristics of methane-air mixtures and those of the respective hybrid mixtures of variable dust concentration originated from Corax N550 and Printex XE2 respectively. Each hybrid mixture case (see x-axis) is represented by two bordered bars, one corresponding to the average explosion parameters of pure methane-air (bars with dense lines) and the second to the average explosion parameters measured in the respective hybrid mixture (bars with medium lines).

For the hybrid mixtures tested in this work, only the methane content is described by the equivalence ratio. One feature noted from this work however, is that the explosion severity changes with the dominant particle size and thus can be increased for low concentrations where nano-sizes are dominant. Hence the effect is not necessarily related to any changes in stoichiometry caused by the addition of carbon particles. The dispersion of carbon-based ENMs into methane-air mixtures potentially resulted in the modification of the chemistry of the combustion reaction. Torrado et al. (2017), applied the micro gas-chromatography method for measurements of the volume fractions of the burnt gases produced by the combustion under quiescent conditions of hybrid mixtures consisting of methane-air at different equivalence ratios and dispersions of low amounts of the two types of nanopowders used here. They reported that the presence of a CB dust cloud affects the combustion reaction, even if the amount of solid fuel is negligible with respect to the methane volume fraction. Especially for lean methane mixtures ($\varphi<0.8$), the conversion of CO to CO_2 was shown to be promoted by the presence of the carbon-based nanomaterial particles, resulting in the increase of explosion severity.

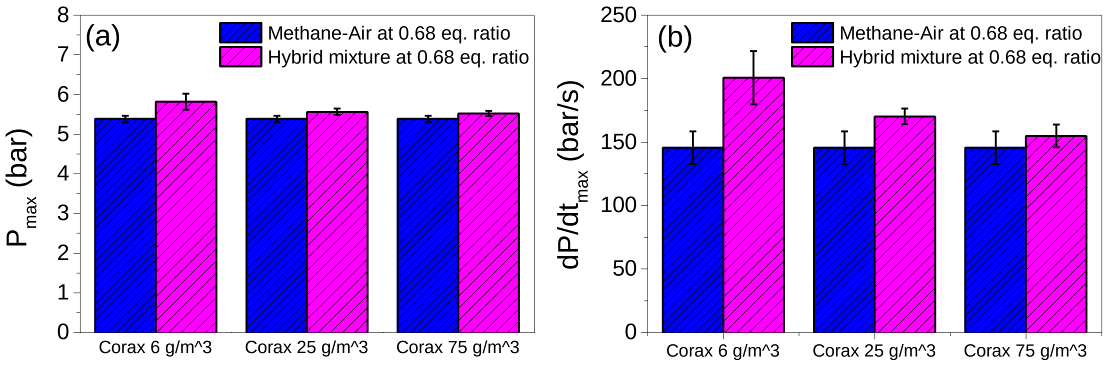

Fig. 10: Comparison of (a) maximum pressure (Pmax) and (b) maximum rate of pressure rise ($(dP/dt)_{max}$), between methane-air mixtures and their respective Corax N550 hybrid mixtures of variable dust concentration (error bars: data $\pm 2\sigma$).

As shown in Fig. 10a, the mixing of Corax N550 into methane-air did not significantly modify the P_{max} of the gas-air mixture. However, significant changes can be observed in the $(dP/dt)_{max}$ as a function of the powder concentration in the mixture (Fig. 10b). The highest influence on $(dP/dt)_{max}$ can be observed at the lowest dust concentration (6 gm^{-3}) hybrid mixture. More specifically, the $(dP/dt)_{max}$ was significantly increased, by around 27.5 % (from 145 bar/s to 200 bar/s), on the addition of 6 gm^{-3} Corax N550. By increasing dust concentration, it was shown that the burning rate gradually decreased until the highest dust concentration (75 gm^{-3}), where the parameter became slightly higher than that demonstrated by the pure methane-air mixture.

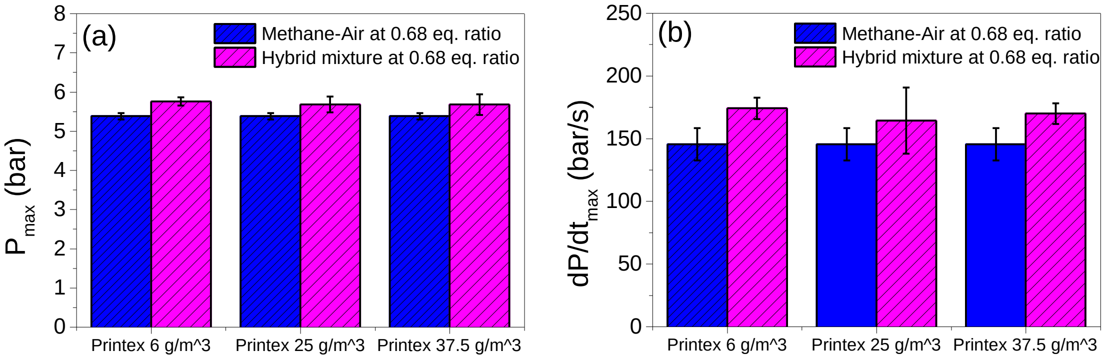

Fig. 11: Comparison of (a) maximum pressure (Pmax) and (b) maximum rate of pressure rise (dP/dt_{max}), between methane-air mixtures and their respective Printex XE2 hybrid mixtures of variable dust concentration(error bars: data ±2σ).

Similarly to Corax N550, the addition of Printex XE2 to methane-air mixtures resulted in slight increases in P_{max} independent of the dust concentration (Fig. 11a). Regarding the $(dP/dt)_{max}$ parameter, it is shown that the methane burning rate was significantly increased by the presence of Printex XE2 particles in the mixture (Fig. 11b). However, in contrast to Corax N550, the level of increase of $(dP/dt)_{max}$ (approximately 16 %) was independent of the dust concentration, indicating that the presence of the suspended particles equivalently affected the explosion characteristics of the tested hybrid mixtures for the reasons discussed below.

The average Schlieren derived flame speeds are plotted against time in Fig. 12 for methane-air and their respective hybrid mixtures of variable dust concentration. The data displayed in the graphs represent polynomial fits to the average flame speed data as calculated by the Schlieren images. The original data has been omitted for the purpose of clarity, although its standard deviations are included to illustrate the variability between the three replicates. Also, it should be noted that the profile of the data shows a decrease during the first milliseconds of the explosion followed by an increase corresponding to the normal development of flame. This is because there is a short transition period following spark ignition in which the initial high energy provided by the spark dissipates to be subsequently superseded by chemical reaction (Gillespie et al., 2000).

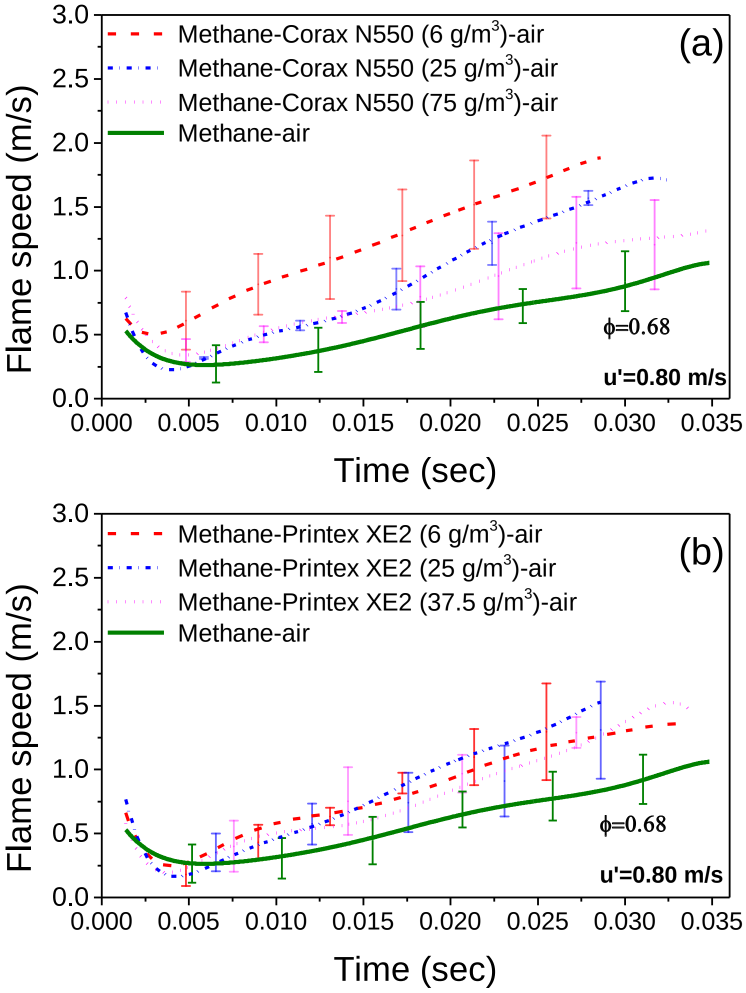

Fig. 12: Variation in the average Schlieren flame speed with time on (a) the variable dust concentration methane-Corax N550-air and methane-air mixtures, and (b) the variable dust concentration methane-Printex XE2-air and methane-air mixtures (error bars: data ± 2σ, line: polynomial fit).

The ignition of hybrid mixtures suspended with 6 gm^{-3} of Corax N550 demonstrated the fastest flame propagation among the total number of the tested hybrid mixtures (Fig. 12a). By increasing the powder concentration into methane-air mixtures, more modest increases in flame speed were induced, compared to that observed for the lowest dust concentration. Also, the increase in the flame speed induced by the addition of 25 gm^{-3} of Corax N550 was higher than that induced by the addition of 75 gm^{-3}.

The addition of Printex XE2, similarly to Corax N550, resulted in higher flame speeds than those of the particle-free mixture (Fig. 12b). However, in comparison to Corax N550, the induced average increase of the flame speed by the suspended powder was slightly lower. This could be attributed to the different particle size characteristics in the dust clouds produced by the dispersion of each material. As indicated by the DMS measurements, the suspended μm particles in the Printex XE2 dust clouds were noted to have larger diameters and more intense presence compared to those in the Corax N550 ones.

The combustion of μm size particles is a process which occurs heterogeneously (Lemkowitz and Pasman, 2014). This process involves many sequential stages, where one of the factors influencing this process is the particle size (larger airborne particles need more time to be exposed to heat to be totally burnt compared to the smaller ones). Therefore, it is possible that the heat released from the flame front was not sufficiently energetic to quickly ignite the surrounding coarser fractions of Printex XE2. As a result, the flame growth in the Printex XE2 cloud was slower than that observed in the Corax N550 cloud.

It is interesting to note that both measurement techniques employed by this work for the characterisation of the explosion violence in the tested mixtures, indicated that the dispersion of the lowest dust concentration (6 gm^{-3}) of Corax N550 in methane-air, resulted in the highest increase in explosion violence among the tested hybrid mixtures. Therefore, there seems to be agreement between the estimations of the two measurement techniques. Furthermore, the particle size characterisation conducted in the tested clouds, indicated that the highest fraction of ultrafine particles was released by the dispersion of the lowest dust concentration of Corax N550 (6 gm^{-3}). This suggests that there is a connection between the fraction of ultrafine particles in the dust cloud and the explosion severity of the respective hybrid mixture.

The work of Moussa et al. (2015) suggested that in a burning dust cloud, the calculated flame speed due to radiation in the nanoscale, is approximately one order of magnitude higher than that in the microscale. In other work conducted by Liberman et al. (2015), the simulations in dust clouds consisting of hydrogen gaseous mixtures suspended with fine particles indicated that the radiative preheating of the mixture ahead of the flame, was dependent on the size distribution characteristics of the dispersed particles. As the authors outlined, the consequence of the radiative preheating is the increase of flame propagation. Given that in a dust cloud there are mechanisms such as coagulation taking place that alter the particle size characteristics over time, and that the coagulation rates are proportional to the second power of the total PNC (Hinds, 2012), ultrafine particles, due to their higher mobility than larger particles, have been reported by Rim et al. (2012) to have longer life times in a dust cloud with low PNC compared to those in a dust cloud with high PNC. As a result, there are higher possibilities for the former than for the latter, to be involved in the flame propagation process. Considering the above and the particle size characteristics determined by the DMS measurements, the study confirms a strong association between the presence of ultrafine particles and the explosion severity of a hybrid mixture.

3.4 ***Explosions with methane (φ<LFL) and dispersed amounts of CB*** **nanopowders**

A final series of explosion tests was conducted on hybrid mixtures with gas mixtures below the LFL of methane (φ=0.65). Under these equivalence ratios, the highest nominal dust concentrations of each selected material, among those three tested in the previous tests were injected in order to study the ignition potential of mixtures below the LFL through the spark plug. Additionally, pyrotechnic matches were used as supplementary ignitors in order to study the effect of a higher ignition energy on the explosion characteristics of the same hybrid mixtures, as well as to study the potential for further extension of their ignitability within the non-explosion region of methane. Fig. 13 illustrates the explosion pressure parameters, P_{max} and $(dP/dt)_{max}$, derived from these tests. The standard deviations are also illustrated for replicates that ignited at least twice.

As indicated in the introduction, prior work conducted by Kosinski et al. (2013) reported that ignition below the flammability limit of propane with dispersions of CB dust was impossible due to the negligible amounts of volatiles in the nanopowder. On the contrary, the work presented here indicates that in a relatively isotropic tubulent environment, the ignition of methane below its LFL could be feasible through the dispersion of CB nanopowder.

The explosion parameter affected most by the decrease of equivalence ratio is the $(dP/dt)_{max}$. The results also indicate that the addition of Corax N550 into the gas mixture resulted in the combustion of the mixture at φ=0.55, when the spark plug was used for ignition. However, the ignition of gas at the same equivalence ratio was impossible to achieve by the addition of Printex XE2. As indicated in previous results, the slower flame growths observed in the Printex XE2 dust clouds compared to those in the Corax N550 ones was attributed to the strong presence of large μm-agglomerates in the former. Therefore, according to the above it is concluded that as the mean particle size decreases, a hybrid mixture of an extremely low content of flammable gas could be ignitable.

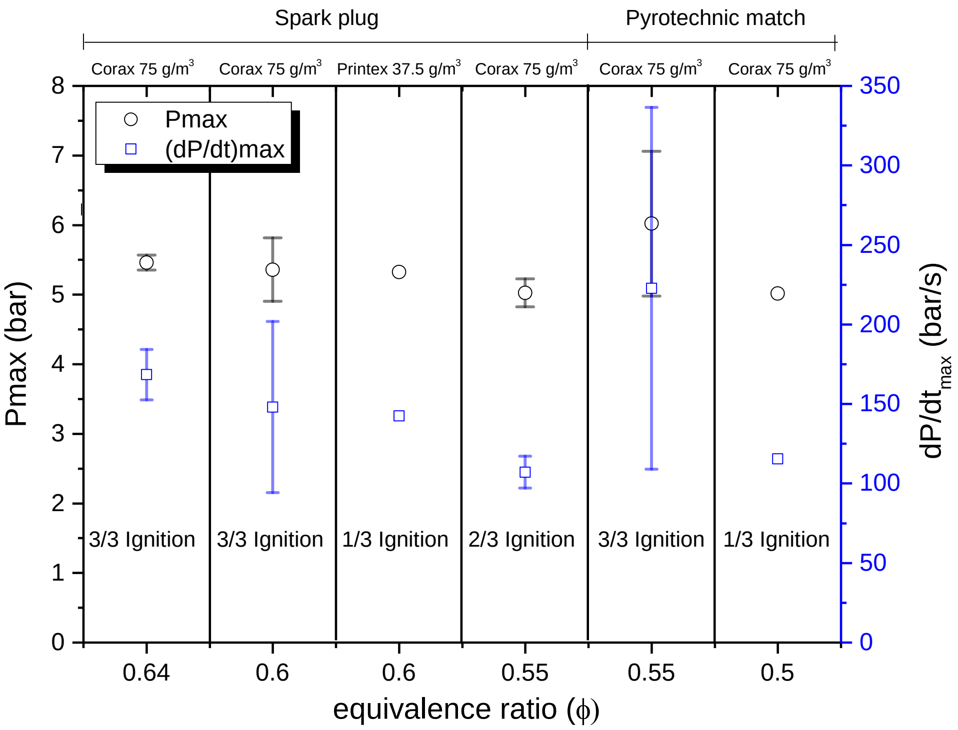

Fig. 13: The average explosion pressure characteristics of hybrid mixtures below the flammability limit of methane (error bars: data ± 2σ).

Another interesting feature in Fig. 13 is the high standard deviation estimated between the replicates at φ=0.60 for the Corax N550 hybrid mixture. This indicates that the severity of explosion at very low equivalence ratios could be very violent and unpredictable in a hybrid mixture with suspended amounts of a nanopowder. It is possible that as the methane content is reduced then the explosion phenomenology of mixture relies more on the particle combustion process than on the gas.

With the application of pyrotechnic matches, for the lowest equivalence ratio (φ=0.50) tested in this work, the mixture was ignitable. Therefore, the application of a moderately higher ignition energy than that of the spark plug, led to the ignition of a hybrid mixture with extremely low content in the flammable gas. According to Billinge (1979), in industrial ignition incidents, a medium energy ignition by friction (approximately 1 kJ) can be caused by 25 kg of powder falling 4 m. This suggests that the ignition energy utilised by the pyrotechnic match (67 J) is significantly lower than that which describes a medium energy ignition in real-life applications. Therefore, the pyrotechnic match simulates ignitions which could potentially occur in the real world when accidentally released fractions of ENMs are mixed with methane and air under atmospheric conditions.

Finally, as shown in Fig. 13, for the same hybrid mixtures (φ=0.55) ignited by the spark plug and the pyrotechnic match, a significant increase in both the explosion pressure parameters and the standard deviation can be seen, caused by the transition from the spark plug to the pyrotechnic match. The average $(dP/dt)_{max}$ of the same mixture was increased by more than 100 % by the use of the pyrotechnic matches (from 107 bar/s to 222 bar/s), while a 20 % increase can be observed in the P_{max} parameter (from 5 bar to 6 bar).

The role of ignition energy on the explosion parameters of gas-air (Hertzberg et al., 1988), dust-air (Hertzberg et al., 1988; Pilão et al., 2006) and gas-dust-air (Di Benedetto et al., 2011; Landman, 1995) has been studied. Strong ignitors applied in small volume vessels have been proven to overdrive the explosion characteristics of homogeneous and heterogeneous mixtures. Therefore, similar to the aforementioned studies, this work suggests that the data obtained from explosions tests conducted through volumetric ignition systems, such as pyrotechnic matches and chemical igniters, should be carefully considered when these are conducted in small vessels. This can possibly lead to overestimation of the average measured explosion characteristics and misinterpretations of the science.

4. Conclusions

The effects of the dispersion of determined amounts of selected CB nanopowders on the explosion characteristics of lean methane-air mixtures, have been experimentally studied in centrally ignited spherical turbulent flames. Comparison of results was made with those for turbulent gaseous flames. From a risk assessment and prevention point of view, these results may have great significance for processes where ENMs are utilised to enhance the efficiency of established techniques applied in industry.

The dispersion of CB nanopowders under turbulent conditions in lean methane-air mixtures resulted in more severe explosions than that of the gas alone. Interestingly, it was shown that among the hybrid mixtures of variable dust concentration, the mixture of the highest fraction of ultrafine particles demonstrated the strongest effects on the explosion severity. At the same time, the particular mixture was that of the lowest dust concentration. Therefore it is concluded that the accidental release in air of a relatively minor amount of nanopowder combined with a low amount of a flammable gas and an electrostatic spark, can result in a severe explosion with consequences for humans and installations potentially higher than those occurred from a higher amount. This work also demonstrated that a nanopowder-based hybrid mixture can be ignitable through an accidental electrostatic spark at an equivalence ratio well below the LFL of the flammable gas, despite its low content of volatiles. However, between two dust clouds of different agglomeration state, the cloud with the lowest presence of μm particles demonstrated the highest extension below the LFL of the gas. Therefore, it can be concluded that as the mean particle size decreases, a hybrid mixture of an extremely low content of gas could be ignitable.

Finally, the present work introduced the application of an optical technique (Schlieren system) for the determination of flame speed in ignited nanopowder-based hybrid mixtures. The Schlieren-derived flame speed measurements identified the severest explosion for the same mixture as that indicated by the traditional method based on the explosion pressure measurements. Therefore, since the burning rates derived from pressure traces are vessel dependent (Vissotski et al., 2012), the former can be used as an alternative tool for direct measurements of the flame velocity less dependent on the facility and more on the reactive properties of the fuel and oxidiser.

Acknowledgments

The authors would like to thank the European Commission 7th Framework program for Research and Technological Development NMP under grant agreement FP7-NMP-2010-LARGE-4, № 263215, the French Ministry of Ecology, Energy Transport and Sustainable Development and the French Ministry of Research for their fruitful collaborations.

References

Abdel-Gayed, R.G., Bradley, D., McMAHON, M., 1979. Turbulent flame propagation in premixed gases: theory and experiment, Symposium (International) on Combustion. Elsevier, pp. 245-254.

Abdelsalam, E., Samer, M., Attia, Y., Abdel-Hadi, M., Hassan, H., Badr, Y., 2016. Comparison of nanoparticles effects on biogas and methane production from anaerobic digestion of cattle dung slurry. Renewable Energy 87, 592-598.

Amyotte, P.R., Eckhoff, R.K., 2010. Dust explosion causation, prevention and mitigation: An overview. Journal of Chemical Health and Safety 17, 15-28.

Amyotte, P.R., Pegg, M.J., Khan, F.I., Nifuku, M., Yingxin, T., 2007. Moderation of dust explosions. Journal of Loss Prevention in the Process Industries 20, 675-687.

Atzler, F., 1999. Burning velocities in droplet suspensions, PhD Thesis, School of Mechanical Engineering, University of Leeds.

Atzler, F., Lawes, M., 1998. Burning velocities in droplet suspensions, Proc. 14th Int. Conference On Liquid Atomisation and Spray Systems, pp. 578-583.

Billinge, K., 1979. The frictional ignition hazard in industry-a survey of reported incidents from 1958 to 1978. Fire prevention science and technology 24, 242-250.

Bouillard, J., Crossley, A., Dien, J.-M., Dobson, P., Klepping, T., Vignes, A., 2008. What about explosivity and flammability of nanopowders. Safety Parameters Characterisation Techniques for Nanoparticles. nanoSAFE (Hg.).

Bradley, D., Lung, F.-K., 1987. Spark ignition and the early stages of turbulent flame propagation. Combustion and Flame 69, 71-93.

Cashdollar, K.L., 1996. Coal dust explosibility. Journal of loss prevention in the process industries 9, 65-76.

Cashdollar, K.L., 2000. Overview of dust explosibility characteristics. Journal of Loss Prevention in the Process Industries 13, 183-199.

Cashdollar, K.L., Zlochower, I.A., Green, G.M., Thomas, R.A., Hertzberg, M., 2000. Flammability of methane, propane, and hydrogen gases. Journal of Loss Prevention in the Process Industries 13, 327-340.

Di Benedetto, A., Garcia-Agreda, A., Russo, P., Sanchirico, R., 2011. Combined effect of ignition energy and initial turbulence on the explosion behavior of lean gas/dust-air mixtures. Industrial & Engineering Chemistry Research 51, 7663-7670.

Dufaud, O., Perrin, L., Traore, M., Chazelet, S., Thomas, D., 2009. Explosions of vapour/dust hybrid mixtures: a particular class. Powder Technology 190, 269-273.

Eckhoff, R.K., 2003. Dust explosions in the process industries: identification, assessment and control of dust hazards. Gulf professional publishing.

Eckhoff, R.K., 2012. Does the dust explosion risk increase when moving from µm-particle powders to powders of nm-particles? Journal of Loss Prevention in the Process Industries 25, 448-459.

Garcia, A., Di Benedetto, A., Russo, P., Salzano, E., Sanchirico, R., 2011. Dust/gas mixtures. Study of hybrid mixture explosions. Powder Technol. 205, 81-86.

Gillespie, L., Lawes, M., Sheppard, C., Woolley, R., 2000. Aspects of laminar and turbulent burning velocity relevant to SI engines. SAE Technical Paper.

Hansen, S.F., 2010. A global view of regulations affecting nanomaterials. Wiley Interdisciplinary Reviews: Nanomedicine and Nanobiotechnology 2, 441-449.

Hertzberg, M., Cashdollar, K.L., Zlochower, I.A., 1988. Flammability limit measurements for dusts and gases: ignition energy requirements and pressure dependences, Symposium (international) on combustion. Elsevier, pp. 303-313.

Hinds, W.C., 2012. Aerosol technology: properties, behavior, and measurement of airborne particles. John Wiley & Sons.

Khalili, I., Dufaud, O., Poupeau, M., Cuervo-Rodriguez, N., Perrin, L., 2012. Ignition sensitivity of gas–vapor/dust hybrid mixtures. Powder technology 217, 199-206.

Kosinski, P., Nyheim, R., Asokan, V., Skjold, T., 2013. Explosions of carbon black and propane hybrid mixtures. Journal of Loss Prevention in the Process Industries 26, 45-51.

Kuriechan, S., 2005. Causes and impacts of accidents in chemical process industries and a study of the consequence analysis software. MPhil Thesis, Pondicherry University.

Kylafis, G.F., 2016. The Explosion and Dispersion Potential of Engineered Nanoparticles, PhD thesis. University of Leeds. Available at: http://etheses.whiterose.ac.uk/15618/.

Landman, G., 1995. Ignition behaviour of hybrid mixtures of coal dust, methane, and air. Journal of the Southern African Institute of Mining and Metallurgy 95, 45-50.

Lawes, M., 1987. Effects of turbulence on combustion in engines PhD thesis, University of Leeds

Lemkowitz, S.M., Pasman, H.J., 2014. A Review of the Fire and Explosion Hazards of Particulates. KONA Powder and Particle Journal 31, 53-81.

Liberman, M., Ivanov, M., Kiverin, A., 2015. Effects of thermal radiation heat transfer on flame acceleration and transition to detonation in particle-cloud hydrogen flames. Journal of Loss Prevention in the Process Industries 38, 176-186.

Liu, Y., Sun, J., Chen, D., 2007. Flame propagation in hybrid mixture of coal dust and methane. Journal of Loss Prevention in the Process Industries 20, 691-697.

Lu, Y.-F., Chou, F.-C., Lee, F.-C., Lin, C.-Y., Tsai, D.-H., 2016. Synergistic Catalysis of Methane Combustion Using Cu–Ce–O Hybrid Nanoparticles with High Activity and Operation Stability. The Journal of Physical Chemistry C 120, 27389-27398.

Mansour, M.S., 2010. Fundamental study of premixed combustion rates at elevated pressure and temperature. University of Leeds.

Moussa, R.B., Guessasma, M., Proust, C., Saleh, K., Fortin, J., 2015. Thermal radiation contribution to metal dust explosions. Procedia Engineering 102, 714-721.

Pilao, R., Ramalho, E., Pinho, C., 2006. Explosibility of cork dust in methane/air mixtures. Journal of loss prevention in the process industries 19, 17-23.

Pilão, R., Ramalho, E., Pinho, C., 2006. Overall characterization of cork dust explosion. Journal of hazardous materials 133, 183-195.

Pritchard, D., 2004. Literature review: explosion hazards associated with nanopowders. Health and Safety Laboratory.

Rim, D., Green, M., Wallace, L., Persily, A., Choi, J.-I., 2012. Evolution of ultrafine particle size distributions following indoor episodic releases: relative importance of coagulation, deposition and ventilation. Aerosol Science and Technology 46, 494-503.

Seipenbusch, M., Binder, A., Kasper, G., 2008. Temporal evolution of nanoparticle aerosols in workplace exposure. Annals of occupational hygiene 52, 707-716.

Sick, V., 2013. High speed imaging in fundamental and applied combustion research. Proceedings of the Combustion Institute 34, 3509-3530.

Torrado, D., Cuervo, N., Pacault, S., Dufour, A., Glaude, P., Murillo, C., Dufaud, O., 2016. Explosions of gas/carbon black nanoparticles mixtures: an approach to assess the role of soot formation. Chem. Eng. Trans. 48, 379-384.

Torrado, D., Glaude, P.-A., Dufaud, O., 2017. Effect of carbon black nanoparticles on methane/air explosions: Influence at low initial turbulence, Journal of Physics: Conference Series. IOP Publishing, p. 012022.

Turkevich, L.A., Dastidar, A.G., Hachmeister, Z., Lim, M., 2015. Potential explosion hazard of carbonaceous nanoparticles: Explosion parameters of selected materials. Journal of hazardous materials 295, 97-103.

Vijayaraghavan, G., 2004. Impact assessment, modelling, and control of dust explosions in chemical process industries. MTech Thesis, Department of Chemical Engineering, Coimbatore Institute of Technology.

Vissotski, A.J., Camou, A., Mannan, S., Petersen, E., 2012. Development of an Experimental Facility for Flame Speed Measurements in Powdered Aerosols. Texas A & M University.

Worsfold, S.M., Amyotte, P.R., Khan, F.I., Dastidar, A.G., Eckhoff, R.K., 2012. Review of the explosibility of nontraditional dusts. Industrial & Engineering Chemistry Research 51, 7651-7655.

Zhen, G., Leuckel, W., 1997. Effects of ignitors and turbulence on dust explosions. Journal of Loss Prevention in the Process Industries 10, 317-324.